European Biophysics Journal (2022) 51:1–13
https://doi.org/10.1007/s00249-021-01581-x

EBSA
Biophysics in Europe

REVIEW

Mechanical waves caused by collective cell migration: generation

Ivana Pajic-Lijakovic[1] · **Milan Milivojevic**[1]

Received: 24 April 2021 / Revised: 30 June 2021 / Accepted: 4 December 2021 / Published online: 24 January 2022

Abstract
Long-timescale viscoelasticity caused by collective cell migration (CCM) significantly influences cell rearrangement and induces generation of mechanical waves. The phenomenon represents a product of the active turbulence occurring at low Reynolds number. The generation of mechanical waves has been a subject of intensive research primarily in 2D multicellular systems, while 3D systems have not been considered in this context. The aim of this contribution is to discuss the generation of mechanical waves during 3D CCM in two model systems: (1) the fusion of two-cell aggregates and (2) cell aggregate rounding after uni-axial compression, pointing out that mechanical waves represent a characteristic of CCM in general. Such perturbations are also involved in various biological processes, such as embryogenesis, wound healing and cancer invasion. The inter-relation between the viscoelasticity and the appearance of active turbulence remains poorly understood even in 2D. The phenomenon represents a consequence of the competition between the viscoelastic force and the surface tension force which induces successive stiffening and softening of parts of multicellular systems. The viscoelastic force is a product of the residual cell stress accumulation and its inhomogeneous distribution caused by CCM. This modeling consideration represents a powerful tool to address the generation of mechanical waves in CCM towards an understanding of this important but still controversial topic.

Keywords Collective cell migration · Cell mobility · The state of viscoelasticity · Cell residual stress accumulation · Effective inertia · The active turbulence

Introduction

Collection cell migration (CCM) within multicellular systems induces spontaneous generation of mechanical waves (Serra-Picamal et al. 2012; Tambe et al. 2013; Notbohm et al. 2016; Pajic-Lijakovic and Milivojevic 2020b; Petrolli et al. 2021). A more comprehensive account of oscillatory patterns generation is essential for a wide range of biological processes such as morphogenesis, wound healing, regeneration, and cancer invasion (Blanchard et al. 2019; Barriga and Mayor 2019; Pajic-Lijakovic and Milivojevic 2019a, 2020a). A term mechanical waves is used to identify all periodical fluctuations of mechanical parameters, such as: (1) cell velocity, (2) the resulting strain rate, (3) the rate of surface, volume, shape and curvature change of multicellular systems, and (4) the stress change. These changes are accompanied with local stiffening and softening of multicellular systems during CCM. The generation of mechanical waves has been experimentally confirmed during flow of various soft matter systems under low Reynolds number (R_e) such as polymer liquids and melts (Groisman and Steinberg 1998, 2000) and has been recognized in experiments with 2D CCM. The oscillatory, wave-like motion of the system constituents represents a consequence of their viscoelasticity which accounts for the stress relaxation and residual stress accumulation (Groisman and Steinberg 2000; Pajic-Lijakovic and Milivojevic 2020b). Normal cell residual stress is accumulated during (1) movement of cell clusters through dense surrounding and (2) collision of cell velocity fronts caused by uncorrelated motility (Pajic-Lijakovic and Milivojevic 2020a, 2021a). Shear residual stress is accumulated primarily at the biointerface between migrating cell clusters and surrounding cells in the resting state (Pajic-Lijakovic and Milivojevic 2020a). Cell movement induces local generation of strain and its long-time change. The strain leads to generation of stress its short-time relaxation during successive short-time relaxation cycles and the long-time

✉ Ivana Pajic-Lijakovic
iva@tmf.bg.ac.rs

[1] Faculty of Technology and Metallurgy, Belgrade University, Belgrade, Serbia

residual stress accumulation (Pajic-Lijakovic and MIlivojevic 2019a). Short-time scale corresponds to minutes, while the long-time scale corresponds to hours. Inhomogeneous distribution of the cell residual stress leads to a generation the viscoelastic force which acts to suppress CCM (Pajic-Lijakovic and Milivojevic 2020b). Corresponding structural changes induces a long-time effective inertia in the context of local forward and backward flows (Notbohm et al. 2016; Pajic-Lijakovic and Milivojevic 2020b). The phenomenon is called "the elastic turbulence" (Groisman and Steinberg 1998, 2000). The elastic turbulence is quantified by Weissenberg number $W_i = \frac{v\tau_R}{L}$ (where τ_R is the stress relaxation time, v is the velocity, L is the characteristic length). In contrary to other viscoelastic soft matter systems, cells show active responses under various experimental conditions with ability of self-adaptation and tendency to control their environment by various biochemical processes such signaling and gene expression. Consequently, the mechanical waves generation during CCM represents a product of "active turbulence" (Alert et al. 2021). Deeper understanding of long-time viscoelasticity of multicellular systems caused by CCM is necessary to understand the active turbulence.

The viscoelasticity caused by CCM has been considered based on several 2D and 3D modeling systems such as: (1) free expansion of cell monolayers (Serra-Picamal et al. 2012; Nnetu et al. 2012), (2) cell swirling motion within confluent monolayers (Notbohm et al. 2016), (3) cell aggregate micropipette aspiration (Guevorkian et al. 2011), (4) cell aggregate uni-axial compression between parallel plates (Mombach et al. 2005; Marmottant et al. 2009; Pajic-Lijakovic 2017a), and (5) fusion of two-cell aggregates (Shafiee et al. 2015; Dechristé et al. 2018; Oriola et al. 2020; Ongenae et al. 2021). Pérez-González et al. (2019) discussed the cell monolayer shape fluctuations by formulating the active wetting model at a cellular level. The 2D shape fluctuations represent the result of competition between cell traction force and contractile intercellular stress which has a feedback impact on the tissue morphology. The fluctuation of spreading velocity described by Pérez-González et al. (2019), as well as the generation of forward and backward cell flows during the monolayer free expansion discussed by Serra-Picamal et al. (2012) and inward and outward cell flow during cell swirling motion considered by Notbohm et al. (2016) confirm the existence of the effective inertial effects that occur under low Reynolds number (Notbohm et al. 2016; Pajic-Lijakovic and MIlivojevic 2020b). Significant attempts have been made to describe the main characteristics of mechanical waves by considering 2D multicellular systems (Serra-Picamal et al. 2012; Notbohm et al. 2016). However, 3D modeling systems also show periodical changes of mechanical parameters during a long-term cell rearrangement.

Guevorkian et al. (2011) discussed long-timescale shivering during the aggregate micropipette aspiration with a period of oscillation of 20 min. This time scale corresponds to cell persistence time (Mc Cann et al. 2010) and accounts for cumulative effects of cell contractions, while single-cell contractions and cell shape relaxation corresponds to a time scale of minutes. Pajic-Lijakovic and Milivojevic (2017a) considered cell aggregate rounding after uni-axial compression. They revealed that the aggregate shape free relaxation shows periodical pattern in the form of successive relaxation cycles of the cell aggregate shape. The phenomenon is similar to the cell monolayer shape fluctuations discussed by Pérez-González et al. (2019). The relaxation rates are not random but gather around two or three values indicating various scenarios of cell migration. These scenarios have been related with the configuration of migrating cells (Pajic-Lijakovic and Milivojevic 2017a). Three scenarios of cell migration were discussed as (1) most of the cells migrate, (2) most of the cells stay in the resting state, and (3) some cell groups migrate while the others, at the same time, stay in resting state (Pajic-Lijakovic and Milivojevic 2017a). The single cycle duration varied from 20 min to 1.5 h depending on cell type and experimental conditions (Pajic-Lijakovic and Milivojevic 2017a). The fusion of cell aggregates has not been considered in the context of the mechanical waves generation. The main goal of this theoretical consideration is to discuss the oscillatory phenomena obtained during (1) the fusion of two-cell aggregates and (2) cell aggregate rounding after uni-axial compression.

Two types of mechanical waves have been recognized in 2D multicellular systems, i.e. standing waves and propagative waves. Standing waves were generated in a confined environment (Deforet et al. 2014; Notbohm et al. 2016; Petrolli et al. 2021) while the propagative waves were generated during monolayer free expansion by traveling through the system (Serra-Picamal et al. 2012; Tlili et al. 2018; Petrolli et al. 2021). The standing waves represent a characteristic of local cell rearrangement which leads to swirling motion (Notbohm et al. 2016; Pajic-Lijakovic and Milivojevic 2020b). The main characteristics of standing waves are (1) the radial velocity and cell tractions are uncorrelated, (2) radial stress component σ_{crr} and the corresponding strain rate $\dot{\varepsilon}_{crr}$ are uncorrelated, (3) radial stress component is simultaneously tensional and compressional, and (4) time derivative of the stress component is in a phase with the corresponding strain rate (Notbohm et al. 2016; Petrolli et al. 2021). The main characteristics of propagative waves are that (1) normal stress component σ_{cxx} and corresponding strain rate $\dot{\varepsilon}_{cxx}$ are in phase quadrature, (2) normal stress component is always tensional, and (3) velocity and cell tractions are uncorrelated (Serra-Picamal et al. 2012; Petrolli et al. 2021). Until now, little is reported about influence of the monolayer viscoelasticity on propagation of mechanical waves. Tambe et al. (2013), Serra-Picamal et al. (2012), Notbohm et al. (2016) treated a monolayer as homogeneous, isotropic and elastic. On that base, they neglected inertial effects during

CCM. However, an inhomogeneous distribution of the cell residual stresses induces generation of the viscoelastic force is responsible for appearance of the effective inertia (Pajic-Lijakovic and Milivojevic 2019a, 2020b). The cell long-term rearrangement is driven by the surface tension force in one hand and the viscoelastic force on the other. Permanent action of these forces induces generation of the mechanical waves in all 2D and 3D modeling systems. The generation of mechanical waves during: (1) a fusion of two-cell aggregates and (2) cell aggregate rounding after uni-axial compression will be discussed based on experimental data from the literature.

The main characteristics of mechanical waves

Mechanical waves represent periodical changes of mechanical parameters such as: (1) cell velocity, (2) volumetric and surface strain rates, (3) the rate of cell aggregate shape and curvature change, and (4) stress (Serra-Picamal et al. 2012; Notbohm et al. 2016; Petrolli et al. 2021). This phenomenon of the active turbulence has been recognized during CCM within various modeling multicellular systems. The extensive research has been devoted to study the generation of mechanical waves during 2D CCM of confluent cell monolayers (Notbohm et al. 2016) and during the free expansion of monolayers (Serra-Picamal et al. 2012). However, much less attention was paid to consider the generation of mechanical waves during 3D CCM. The main goal of this paper is to discuss this complex phenomenon obtained during cell aggregate rounding after uni-axial compression and during the fusion of two-cell aggregates.

For these modeling systems, the mechanical waves represent a consequence of long-term cell rearrangement driven by the viscoelastic force and the surface tension force. The viscoelastic force is a resistive force directed always opposite to the direction of migration (Pajic-Lijakovic and Milivojevic 2020b). The surface tension force acts to reduce a surface and represents the driving force for CCM. The competition of these two forces induces successive stiffening and softening of multicellular systems and influences the configuration of migrating cells (Pajic-Lijakovic and Milivojevic 2017a, 2020b). The corresponding force balance is formulated by modifying the model proposed by Pajic-Lijakovic and Milivojevic, (2020b) for 2D CCM and expressed as:

$$n(r,t)\frac{D\vec{v}_c(r,\tau)}{Dt} = n(r,t)\vec{F}_{st}(r,t) - \vec{F}_{Tve}(r,t) \quad (1)$$

where t is the long-timescale for several tens of minutes to hours, $\vec{v}_c$ is the cell velocity equal to $\vec{v}_c(r,t) = \frac{d\vec{u}_c}{dt}$, $\vec{u}_c$ is the cell displacement field, $\frac{D\vec{v}_c}{Dt} = \frac{\partial\vec{v}_c}{\partial t} + (\vec{v}_c \cdot \vec{\nabla})\vec{v}_c$ is the material derivative (Bird et al. 1960), $n(r,t)$ is the cell packing density, $\vec{F}_{st}$ is the surface tension force equal to $\vec{F}_{st}(r,t) = \gamma\vec{u}_c$, γ is the surface tension, $\vec{F}_{Tve}$ is the viscoelastic force equal to $\vec{F}_{Tve}(r,t) = \vec{\nabla} \bullet (\tilde{\sigma}_{Rc})$, while $\tilde{\sigma}_{cR}(r,t)$ is the cell residual stress equal to $\tilde{\sigma}_{cR}(r,t) = \tilde{\sigma}_{cRV}(r,t) + \tilde{\sigma}_{cRS}(r,t)$, $\tilde{\sigma}_{cRV}(r,t)$ is the normal residual stress, and $\tilde{\sigma}_{cRS}(r,t)$ is the shear residual stress.

The surface tension force causes CCM to reduce the surface by (1) cell aggregate rounding after uni-axial compression (Rieu et al. 2000; Mombach et al. 2005; Marmottant et al. 2009) and (2) increasing the neck radius during the fusion of two-cell aggregates (Shafiee et al. 2015; Oriola et al. 2020; Ongenae et al. 2021). CCM is directed from the aggregate surface region to its core region during the cell aggregate rounding. For the case of the cell aggregates fusion, CCM is intensive at the contact point between two-cell aggregates which leads to an increase in the neck radius. In this case, generated two-cell velocity fronts have an opposite directions. Every velocity front is directed from the surface region of one aggregate to the core region of the other. Consequently, local collisions of velocity fronts induce an increase in cell packing density which can lead to the cell jamming state transition (Trepat et al. 2009; Nnetu et al. 2012; Pajic-Lijakovic and Milivojevic 2019c, 2021a). The phenomenon of collision of the velocity fronts and cell jamming state transition was elaborated in 2D CCM by Nnetu et al. (2012). Local cell jamming state transitions near the contact point between two aggregates can induce damping effects of the aggregates fusion (Oriola et al. 2020). This phenomenon known as the "arrested coalescence" depends on (1) the fraction of cells in jamming state within the neck region and (2) the ability of cells to undergo unjamming transition. Consequently, the arrested coalescence depends on cell type and aggregate size. Epithelial-like MCF-10A cell aggregates are prone to arresting coalescence while malignant MDA-MB-436 cells aggregate performs total fusion (Grosser et al. 2021). This interesting result is understandable when we keep in mind that malignant cells can easy change the mode of cell movement depending on microenvironmental conditions and on that base undergo to the unjamming cell state transition. The arrested coalescence could represent a product of inhomogeneous distribution of cell residual stress within a neck region (Pajic-Lijakovic and Milivojevic 2017a).

CCM leads to the residual stress accumulation. The shear and normal residual stresses accumulation induces an increase in the viscoelastic force which results in stiffening of the multicellular system parts (Pajic-Lijakovic and Milivojevic 2019a, 2020a, 2021a). The viscoelastic force reduces cell migration and change the configuration of migrating cells (Pajic-Lijakovic and Milivojevic 2017a, 2019c) which results in softening of the multicellular system parts. This softening leads to a decrease in the cell residual stress and on that base reduces the viscoelastic force (Pajic-Lijakovic and Milivojevic 2020b). Then, CCM starts again, driven by

the tissue surface tension force. Pajic-Lijakovic and Milivojevic (2017a, 2019c) correlated periodic changes of the cell aggregate shape with the configuration of migrating cells during its rounding and recognized periodical jamming-to-unjamming cell state transitions.

The residual stress accumulation can be described based on proposed constitutive model for viscoelastic solid or viscoelastic liquid (Pajic-Lijakovic and Milivojevic 2017b). Ability of volumetric and surface strains to relax under constant stress (or zero stress) conditions represents the characteristic of a viscoelastic solid rather than a viscoelastic liquid (Pajic-Lijakovic 2021). Stress can relax under (1) constant strain conditions for a viscoelastic solid and (2) constant strain rate conditions for a viscoelastic liquid (Pajic-Lijakovic and Milivojevic 2019c).

Viscoelasticity caused by CCM: constitutive models

Mombach et al. (2005) and Marmottant et al. (2009) considered cell aggregate uni-axial compression between parallel plates. They estimated: (1) cell stress relaxation under constant strain (i.e. the aggregate shape) condition, (2) the aggregate shape relaxation under constant stress condition, and (3) the aggregate free relaxation (its rounding) after compression. Ability of aggregate shape, surface, and volume to relax under constant stress (or zero stress) condition represents the characteristic of a viscoelastic solid rather than a viscoelastic liquid (Pajic-Lijakovic 2021). Stress relaxation time corresponds to a time scale of minutes (Marmottant et al. 2009; Pajic-Lijakovic and Milivojevic 2019b). The surface strain relaxation occurs via CCM, and the relaxation time corresponds to a time scale of several tens of minutes to hours (Mombach et al. 2005). For this case, the stress relaxes during successive short-time stress relaxation cycles under constant strain per cycle (Pajic-Lijakovic and Milivojevic 2017a). Recently, Tlili et al. (2020) considered CCM of MDCK cell monolayer and proposed the Maxwell model suitable for viscoelastic liquid. The Maxwell model describes stress relaxation under constant strain rate condition while strain cannot relax (Pajic-Lijakovic 2021). However, Tlili et al. (2020) measured cell velocity distribution and on that base the strain changes rather than stress relaxation ability. They estimated the so called viscous relaxation time equal to 70 ± 15 min which represents cumulative effects of cell shape relaxations. This time scale corresponds rather to the strain relaxation time while the stress relaxation time is much shorter. Ability of strain to relax pointed to the viscoelastic solid rather than viscoelastic liquid.

To estimate the viscoelasticity of two-cell aggregate system during fusion, it is necessary to discuss the system ability to relax. Shafiee et al. (2015) considered fusion of two confluent skin fibroblast cell aggregates and pointed out that the surface of the two-aggregate system decreases and relaxes from 1.2mm^2 to 0.55mm^2 while the volume ratio $\frac{V}{V_0}$ decreases and relaxes from 1 to 0.42 within 140 h (where V_0 is the initial volume of the two-aggregate system and $V(t)$ is its current volume). This result pointed to a viscoelastic solid behavior. Oriola et al. (2020) proposed the Kelvin-Voigt model for describing cell long-timescale rearrangement during the aggregates fusion. This model represents a good choice for describing the viscoelasticity of multicellular system near the cell jamming transition (Pajic-Lijakovic and Milivojevic 2021b). Ongenae et al. (2021) proposed the model for describing the fusion of cell aggregates by pretending to account for the long-term viscoelasticity. They introduced the storage modulus into the model and neglect the loss modulus. It is unclear which constitutive model they applied. Kosztin et al. (2012), Oswald et al. (2017) and Dechristé et al. (2018) treated two-aggregate fusion as a viscoelastic liquid. They introduced two inter-connected arguments: (1) a fusion of cell aggregates is driven by the surface tension and (2) the surface tension represents the characteristic of liquid. We agree that the aggregates fusion is driven by the tissue surface tension. However, the surface tension is not necessarily the characteristic of a liquid. Amorphous viscoelastic solids such as polymer hydrogels and foams also have surface tension (Mondal et al. 2015).

Dechristé et al. (2018) considered the fusion of two human carcinoma cell aggregates (HCT116 cell line) as a consequence of cell divisions within 70 h. The doubling time of HCT116 cells is 18 h (Gongora et al. 2008). Within this time period, cell divisions can be neglected, while the volume change occurs primarily via CCM. The result in the form of the volume ratio $\frac{V}{V_0}$ change vs. time significantly depends on the initial aggregate size. The volume ratio $\frac{V}{V_0}$ of larger aggregates ($500\mu m$ diameter) increases and relaxes from 1 to ~ 1.25 within 18 h (Dechristé et al. 2018). In contrast, the volume ratio $\frac{V}{V_0}$ of smaller aggregates ($300\mu m$ diameter) increases significantly to ~ 1.55 obtained after 18 h without reaching the equilibrium state (Dechristé et al. 2018). This interesting result indicated that surface effects are pronounced for the case of smaller cell aggregates which result in a rapid increase in the system volume accompanied with an intensive energy dissipation characteristic for a viscoelastic liquid. While Shafiee et al. (2015) obtained a decrease in the two-aggregate system volume within 140 h; Dechristé et al. (2018) revealed an increase in the two-aggregate system volume even within first 18 h during fusion. These apparently opposite volumetric effects should be discussed in the context of a volumetric strain and quantified by the Poisson's ratio. Schematic presentation of two modeling systems consider here: (1) fusion of two-cell

aggregates and (2) cell aggregate rounding after uni-axial compression were shown in Fig. 1a,b.

In further consideration, we will discuss two constitutive models frequently mentioned in the literature in the context of viscoelasticity caused by CCM extracted based on the multicellular systems ability to relax, i.e.: (1) the Maxwell model suitable for a viscoelastic liquid (Guevorkian et al. 2011; Lee and Wolgemuth 2011; Pajic-Lijakovic and Milivojevic 2021a) and (2) the Zener model suitable for a viscoelastic solid (Pajic-Lijakovic and Milivojevic 2021a; Pajic-Lijakovic 2021). CCM within streams or weakly connected cell groups can be treated as a viscoelastic liquid (Guevorkian et al. 2011), while strongly connected cell clusters can be treated as a viscoelastic solid (Pajic-Lijakovic and Milivojevic 2021a, 2021b). Multicellular systems are inhomogeneous and both types of viscoelasticity can locally exist during CCM (Pajic-Lijakovic and Milivojevic 2021a). The proposed constitutive models will be discussed in the context of local residual stress accumulation caused by CCM.

The Maxwell model

Single-cell movement within a weakly connected tissue parts induces generation of local shear strain rate $\dot{\tilde{\varepsilon}}_{cS}(r,t)$ equal to $\dot{\tilde{\varepsilon}}_{cS}(r,t)=\frac{1}{2}\left(\overrightarrow{\nabla}\vec{v}_c+\overrightarrow{\nabla}\vec{v}_c^{\,T}\right)$ and local volumetric strain rate $\dot{\tilde{\varepsilon}}_{cV}=(\overrightarrow{\nabla}\bullet\vec{v}_c)\tilde{\boldsymbol{I}}$ (where $\tilde{\boldsymbol{I}}$ is identity tensor) (Pajic-Lijakovic and Milivojevic, 2021a). Both strain rates are supposed to be constant during a short-time relaxation cycle and changes from cycle to cycle. These strain rates induce a generation of corresponding shear and normal cell stresses and their relaxation during short-time relaxation cycles. The Maxwell model, in this case, is expressed as:

$$\tilde{\sigma}_{ci}(r,\tau,t)+\tau_R\dot{\tilde{\sigma}}_{ci}(r,\tau,t)=\eta_i\dot{\tilde{\varepsilon}}_{ci}(r,t) \tag{2}$$

where i accounts for shear or volumetric quantities, τ is the short-time scale (the time scale of minutes), t is the long-timescale (the timescale of several tens of minutes to hours), $\tilde{\sigma}_{ci}$ is the normal or shear stress, $\dot{\tilde{\sigma}}_{ci}=\frac{d\tilde{\sigma}_{ci}}{d\tau}$, $\tilde{\varepsilon}_{ci}$ is the shear or volumetric strain, $\dot{\tilde{\varepsilon}}_{ci}=\frac{d\tilde{\varepsilon}_{ci}}{dt}$ is the strain rate, η_i is the shear or volumetric viscosity, and τ_R is the stress relaxation time. Stress relaxation under constant strain rate $\dot{\tilde{\varepsilon}}_{0i}$ per single short-time relaxation cycle can be expressed starting from the initial condition $\tilde{\sigma}_{ci}(r,\tau=0,t)=\tilde{\sigma}_{0ci}$ as:

$$\tilde{\sigma}_{ci}(r,\tau,t)=\tilde{\sigma}_{0ci}e^{-\frac{\tau}{\tau_R}}+\tilde{\sigma}_{Rci}(r,t)\left(1-e^{-\frac{\tau}{\tau_R}}\right) \tag{3}$$

where $\tilde{\sigma}_{Rci}(r,t)$ is the normal or shear residual stress equal to $\tilde{\sigma}_{Rci}=\eta_i\dot{\tilde{\varepsilon}}_{0ci}$. This finding corresponds to experimental data and modeling consideration by Dechristé et al. (2018).

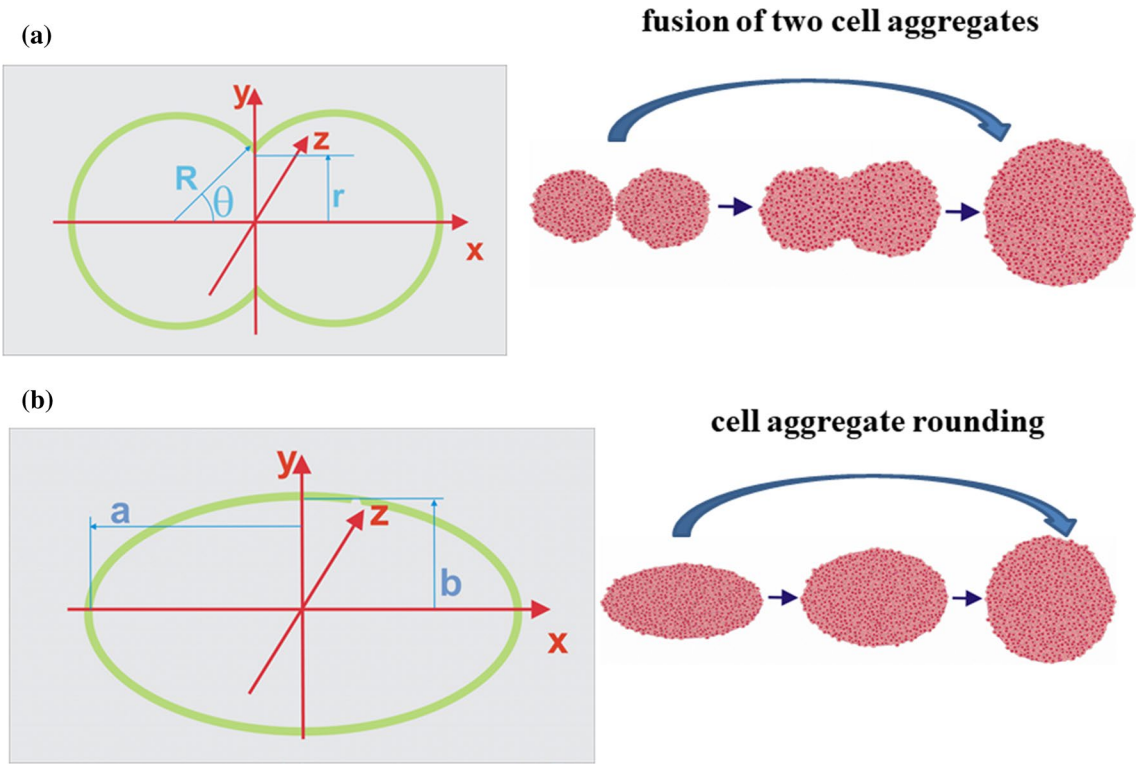

Fig. 1 Schematic presentation of (**a**) fusion of two-cell aggregates and (**b**) cell aggregate rounding after uni-axial compression

The Zener model

The Zener model for a viscoelastic solid is the simplest model which describes: (1) stress relaxation under constant strain conditions and (2) strain relaxation under constant stress condition (Pajic-Lijakovic 2021). Step by step movement of the strongly connected cell cluster through dense surrounding induces generation of local shear strain $\tilde{\boldsymbol{\varepsilon}}_{\boldsymbol{cS}}(r,t)$ and volumetric strain $\tilde{\boldsymbol{\varepsilon}}_{\boldsymbol{cV}}(r,t)$ within the cell clusters. The volumetric compressive strain is also intensive during collision of velocity fronts caused by uncorrelated motility while the shear stress can be intensive at the biointerface between migrating cell clusters and surrounding resting cells (Pajic-Lijakovic and Milivojevic, 2019a, 2021a). For small strain assumption these strains can be expressed as $\tilde{\boldsymbol{\varepsilon}}_{\boldsymbol{cS}} = \frac{1}{2}\left(\vec{\nabla}\vec{\boldsymbol{u}}_c + \vec{\nabla}\vec{\boldsymbol{u}}_c^{\,T}\right)$ and $\tilde{\boldsymbol{\varepsilon}}_{\boldsymbol{cV}} = (\vec{\nabla}\bullet\vec{\boldsymbol{u}}_c)\tilde{\boldsymbol{I}}$ (where $\tilde{\boldsymbol{I}}$ is the unity tensor). These strains are constant per single short-time relaxation cycle and change from cycle to cycle as a result of cell clusters movement (Pajic-Lijakovic and Milivojevic 2020a, 2021a). The strains induce generation of corresponding shear stress $\tilde{\boldsymbol{\sigma}}_{\boldsymbol{cS}}(r,\tau,t)$ and normal (compressive/tensile) stress $\tilde{\boldsymbol{\sigma}}_{\boldsymbol{cV}}(r,\tau,t)$. These stresses relax during short-time relaxation cycles up to residual values $\tilde{\boldsymbol{\sigma}}_{\boldsymbol{cSR}}(r,t)$ and $\tilde{\boldsymbol{\sigma}}_{\boldsymbol{cVR}}(r,t)$, respectively. The Zener model is expressed as (Pajic-Lijakovic and Milivojevic 2020a, 2021a):

$$\tilde{\boldsymbol{\sigma}}_{\boldsymbol{ci}}(r,\tau,t) + \tau_R\dot{\tilde{\boldsymbol{\sigma}}}_{\boldsymbol{ci}}(r,\tau,t) = E_i\tilde{\boldsymbol{\varepsilon}}_{\boldsymbol{ci}}(r,t) + \eta_i\dot{\tilde{\boldsymbol{\varepsilon}}}_{\boldsymbol{ci}}(r,t) \tag{4}$$

where $\tilde{\boldsymbol{\sigma}}_{\boldsymbol{ci}}$ is the shear or normal stress, $\dot{\tilde{\boldsymbol{\sigma}}}_{\boldsymbol{ci}} = \frac{d\tilde{\sigma}_{ci}}{d\tau}$, $\tilde{\boldsymbol{\varepsilon}}_{\boldsymbol{ci}}$ is the shear or volumetric strain, $\dot{\tilde{\boldsymbol{\varepsilon}}}_{\boldsymbol{ci}} = \frac{d\tilde{\varepsilon}_{ci}}{dt}$ is the strain rate, E_i is the shear or Young's elastic modulus, and η_i is the shear or volumetric viscosity, and τ_R is the stress relaxation time. Stress relaxation under constant strain condition $\tilde{\boldsymbol{\varepsilon}}_{\boldsymbol{0ci}}(r,t)$ per single short-time relaxation cycle can be expressed starting from the initial condition $\tilde{\boldsymbol{\sigma}}_{\boldsymbol{ci}}(r,\tau=0,t) = \tilde{\boldsymbol{\sigma}}_{\boldsymbol{0i}}$ as:

$$\tilde{\boldsymbol{\sigma}}_{\boldsymbol{ci}}(r,\tau,t) = \tilde{\boldsymbol{\sigma}}_{0ci}e^{-\frac{\tau}{\tau_R}} + \tilde{\boldsymbol{\sigma}}_{\boldsymbol{Rci}}(r,t)\left(1-e^{-\frac{\tau}{\tau_R}}\right) \tag{5}$$

where $\tilde{\boldsymbol{\sigma}}_{\boldsymbol{Rci}}(r,t)$ is the residual shear or normal stress equal to $\tilde{\boldsymbol{\sigma}}_{\boldsymbol{Rci}} = E_i\tilde{\varepsilon}_{0ci}$.

The surface and volumetric changes induced by CCM

Surface effects of multicellular system lead to an accumulation of the internal normal stress which causes the change of system volume. The internal normal stress represents a product of cumulative effects of local normal residual stress accumulation caused by CCM. The cause-consequence relation between volumetric and surface effects during successive short-time relaxation cycles was expressed by the Young–Laplace equation (Marmottant et al. 2009; Pajic-Lijakovic and Milivojevic 2019c):

$$\sigma_e = \Delta p^j + \sigma_i^j \tag{6}$$

where σ_e is the externally applied stress equal to $\sigma_e = 0$ for the experimental conditions considered here, Δp^j is the hydrostatic pressure during the j-$^{\text{th}}$ relaxation cycle that is equilibrated with the corresponding value of the tissue surface tension γ^j such that $\Delta p^j = \gamma^j H^j$, H^j is the corresponding curvature of the multicellular system equal to $H^j = \left(\frac{dS}{dV}\right)^j$, $S(t)$ is the aggregate surface, $V(t)$ is the aggregate volume, and σ_i is the internal normal residual stress accumulation. The tissue surface tension is in the range from $1\frac{mN}{m}$ to $4\frac{mN}{m}$ (Mombach et al. 2005). Surface tension slowly changes during cell long-timescale rearrangement as a consequence of change the configuration of migrating cells $\gamma = \gamma(configuration)$ (Mombach et al. 2005; Pajic-Lijakovic et al. 2017a).

The internal normal residual stress for the j-th cycle is equal to (Dechristé et al. 2018):

$$\sigma_i^j(t) = \left(\frac{\partial W_V}{\partial \varepsilon_V}\right)^i \tag{7}$$

where $\sigma_i = \sigma_i(\varepsilon_V)$, $W_V(t)$ is the volumetric part of strain energy density equal to: (1) $W_{VZ}(t) = \frac{1}{\Delta V}\int_{\Delta V}\frac{1}{2}\tilde{\boldsymbol{\sigma}}_{\boldsymbol{cRV}} : \tilde{\boldsymbol{\varepsilon}}_{\boldsymbol{cV}}\, d^3r$ for the Zener model and (2) $W_{VM}(t) = \frac{\Delta t}{\Delta V}\int_{\Delta V}\frac{1}{2}\tilde{\boldsymbol{\sigma}}_{\boldsymbol{cRV}} : \dot{\tilde{\boldsymbol{\varepsilon}}}_{\boldsymbol{cV}}\, d^3r$ for the Maxwell model. The total volumetric part of strain energy density is equal to $W_V(t) = X_M(t)W_{VM}(t) + (1-X_M(t))W_{VZ}(t)$ (where $X_M(t)$ is the volume fraction of the mesoscopic domains with the rheological behavior which corresponds to the Maxwell model). The volumetric strain $\varepsilon_V(t)$ is equal to $\varepsilon_V(t) = \frac{dV}{V}$. It accounts for cumulative effects of long-timescale cell rearrangement obtained after short-time stress relaxation cycles. The volume and volumetric strain change during the aggregates fusion should be related to the rheological parameter such as the Poisson's ratio. The volumetric strain accounts for compression in x-direction and extension in y- and z –directions (Fig. 1a,b) expressed as:

$$\varepsilon_V(t) = \left(1+\varepsilon_{xx}\right)\left(1+\varepsilon_{yy}\right)\left(1+\varepsilon_{zz}\right) - 1 \tag{8}$$

where ε_{xx}, ε_{yy}, and ε_{zz} are the diagonal components of strain tensor. Consequently, the strain components are: (1) $\varepsilon_{xx} < 0$ (compression) and (2) $\varepsilon_{yy} > 0$ and $\varepsilon_{zz} > 0$ (extension). For the isotropic extension,y- and z – components are $\varepsilon_{yy} \approx \varepsilon_{zz}$. The compression-to-extension ratio can be quantified by the aspect ratio $AR(t) = \frac{d(t)}{2r(t)}$ (where $d(t)$ is the longer axis and $2r(t)$ is the shorter axis of multicellular system). The longer axis for two-aggregate system during fusion was expressed as: $d(t) = 2R(t)(1+cos\theta)$ while $r(t)$ is the neck radius equal

to: $r(t) = R(t)sin\theta(t)$ (where $R(t)$ is the aggregate radius and $\theta(t)$ is the fusion angle which change from $\theta(0) = 0$ to $\theta(\infty) = \theta_{\infty}$) (Kosztin et al. 2012; Dechristé et al. 2018). The corresponding aspect ratio is equal to $AR(t) = \frac{1+cos\theta}{sin\theta}$. A decrease in the longer axis is induced by compression, while an increase in the shorter axis, at the same time, is induced by extension. The AR increases with time during: (1) the aggregate rounding after uni-axial compression and (2) the fusion of two aggregates. Spherical aggregate shape corresponds to $AR = 1$. The fusion of smaller human carcinoma cell aggregates (HCT116 cell line) leads to a significant extension of two-aggregate systems in y- and z –direction which leads to an increase in the neck radius relative to the diameter of two-aggregate system (Dechristé et al. 2018). For these conditions, the aspect ratio after 18 h is $AR \approx 0.92$ for smaller aggregates, which corresponds to a new ellipsoidal shape. In contrast, the aspect ratio change is slower for larger aggregates and equal to $AR \approx 1.1$ after 18 h (Dechristé et al.2018). Slower dynamics of long-timescale cell rearrangement represents a consequence of pronounced collisions of velocity fronts near the contact point between two aggregates which can lead to the cell jamming state transitions and on that base to the arrested coalescence (Nnetu et al. 2012; Oriola et al. 2020; Grosser et al. 2021). Similar result is obtained for the fusion of two confluent skin fibroblast cell aggregates (Shafiee et al. 2015). The corresponding aspect ratio obtained after 140 h is $AR \approx 1.1$ after 140 h. Mombach et al. (2005) considered rounding of 3D chicken embryonic neural retina aggregate with radius of $143\mu m$. The dynamics of long-timescale cell rearrangement is also slower in comparison with the one caused by the aggregates fusion considered by Dechristé et al. (2018). The corresponding aspect ratio obtained after aggregate shape relaxation within 21 h is $AR \approx 1.52$ (Mombach et al. 2005).

The x-component of the volumetric strain tensor is equal to $\varepsilon_{xx} = -\nu\varepsilon_{yy}$ (where ν is the Poisson's ratio). The total volume increase for the condition $\varepsilon_V(t) > 0$ accompanied with the Poisson's ratio $\nu < 1/2$ (Tschoegl et al. 2002). In contrast, higher value of the Poisson's ratio, i.e. $\nu > 1/2$ leads to the volume decrease. These higher values of the Poisson's ratio pointed to anomalous nature of the system structural changes caused by the mobility reduction of the system constituents. Ban et al. (2019) considered an anomalous Poisson effect during three-axial deformation of the collagen network. Corresponding increase in the Poisson's ratio up to 1.7 is caused by anomalous nature of the collagen filament conformations accompanied with local filament stiffening (Ban et al. 2019). This stiffening reduces a fiber mobility which leads to an increase in the Poisson's ratio. Cell aggregates are much complex than polymer hydrogel networks. However, a decrease in the cell mobility could influence the Poisson's ratio on a similar way. Consequently, a decrease in cell mobility and corresponding increase in cell packing density as well as the normal residual stress (Trepat et al. 2009) can be responsible for a decrease in volume and surface during the fusion of cell aggregates obtained by Shafiee et al. (2015). In contrast, Dechristé et al. (2018) obtained an increase in the volume and surface of the two-aggregate system during fusion within a time period of 18 h in which the cell divisions can be neglected. Total surface of two-aggregate system in contact was expressed as (Kosztin et al. 2012) $S(t) = 4\pi R(t)^2(1 + cos\theta(t))$ while the total volume is (Dechristé et al. 2018): $V(t) = \frac{2\pi}{3}R(t)^3(2 + 3cos\theta(t) - cos^3\theta(t))$. Initial volume of two-aggregate system is $V_0 = \frac{8}{3}\pi R_0^3$, R_0 is the initial single-aggregate radius. The volume can (1) increase for $\frac{V(t)}{V_0} > 1$, (2) stay constant for $\frac{V(t)}{V_0} = 1$, and (3) decrease for $\frac{V(t)}{V_0} < 1$ (Kosztin et al. 2012). The volume decrease is accompanied with an increase in the cell packing density caused by normal residual stress accumulation (Trepat et al. 2009), while the volume increase is accompanied with a decrease in the cell packing density caused by inhomogeneity in the stress distribution. The volume conservation is achieved for the condition $R(t) = 2^{1/3}R_0$ which follows to $V(t) = V_0$. The volume increases for the condition $R(t) > 2^{1/3}R_0$.

The fusion of two-cell aggregates and the generation of mechanical waves

The aggregates fusion induces intensive changes at the contact point between aggregates quantified by an increase in the neck radius from $r(0) = 0$ to $r(t)$ (Fig. 1a). The rate of neck radius change $\frac{dr}{dt}$ during fusion of two human carcinoma cell aggregates (HCT116 cell line) reported by Dechristé et al. (2018) is shown in Fig. 2a. The rate $\frac{dr}{dt}$ vs. time was considered within 18 h which corresponds to a cell doubling time. The rate $\frac{dr}{dt}$ fluctuates around the exponential decrease.

The rate of neck radius change during the fusion of two skin fibroblast cell aggregates reported by Shafiee et al. (2015) is shown in Fig. 2b. For these experimental conditions, the rate $\frac{dr}{dt}$ decreases exponentially with the intensive fluctuations caused by action of the resistive viscoelastic force against the surface tension force.

The periodical change of the curvature of two-aggregate system represents additional confirmation of the generation of mechanical waves during the aggregates fusion. The curvature H is equal to $H = \frac{\sigma_i}{\gamma}$ (from Eq. 6). Consequently, oscillations of the curvature H point to a periodic change of the internal stress-to-surface tension ratio vs. time. The curvature of two human carcinoma cell aggregates (HCT116 cell line)- system change during fusion is shown in Fig. 3a.

The increase in the surface relative to volume and on that base an increase in the curvature H is pronounced for the fusion of smaller cell aggregates (Dechristé et al.

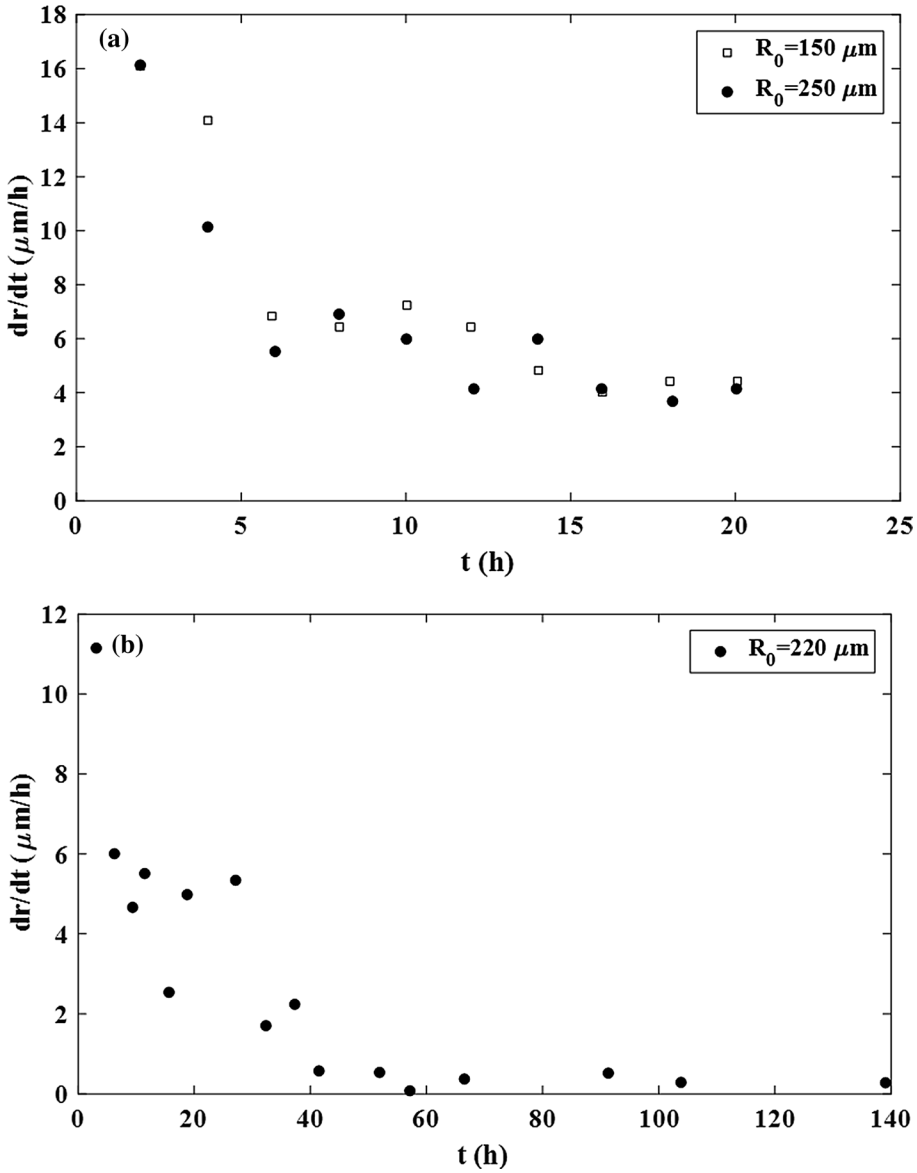

Fig. 2 **a** The rate of change the neck radius during fusion of two human carcinoma cell aggregates (HCT116 cell line). **b** The rate of change the neck radius during fusion of two skin fibroblast cell aggregates

2018). This fusion leads to a significant increase in the neck radius r such that $2r > d$ after 18 h (where d is the longer axis of two-aggregate system). Surprisingly, this multicellular system reaches new ellipsoidal shape rather than being spherical. In contract, the fusion of larger cell aggregates leads to establishing of the approximately spherical shape after 18 h. Local collision of velocity fronts in the region of neck, which causes inhomogeneous distribution of the cell residual stress accumulation, is more intensive in the case of larger aggregates. Consequently, the increase in the curvature H determined for smaller aggregates represents a consequence of cell invasiveness on one hand and the more homogeneous distribution of cell residual stress on the other.

The curvature of two skin fibroblast cell aggregate- system change during fusion is shown in Fig. 3b. Oscillatory trend of the curvature change is recognizable and points to periodical change of the internal stress σ_i and the tissue surface tension γ.

These periodic changes of (1) the rate $\frac{dr}{dt}$ (Fig. 2a, b) and (2) the curvature of two-aggregate systems (Figs. 3a, b) represent a consequence of action the surface tension force which drives the long-timescale cell rearrangement and the viscoelastic force which resists this rearrangement. The accumulation of the cell residual stress and its inhomogeneous distribution during CCM induces an increase in the viscoelastic force and on that base causes the system local stiffening. The viscoelastic force reduces cell migration which leads to a system softening. This system softening results in a decrease in the viscoelastic force. This decrease induces CCM again driven by the surface tension force. These successive stiffening and softening of multicellular

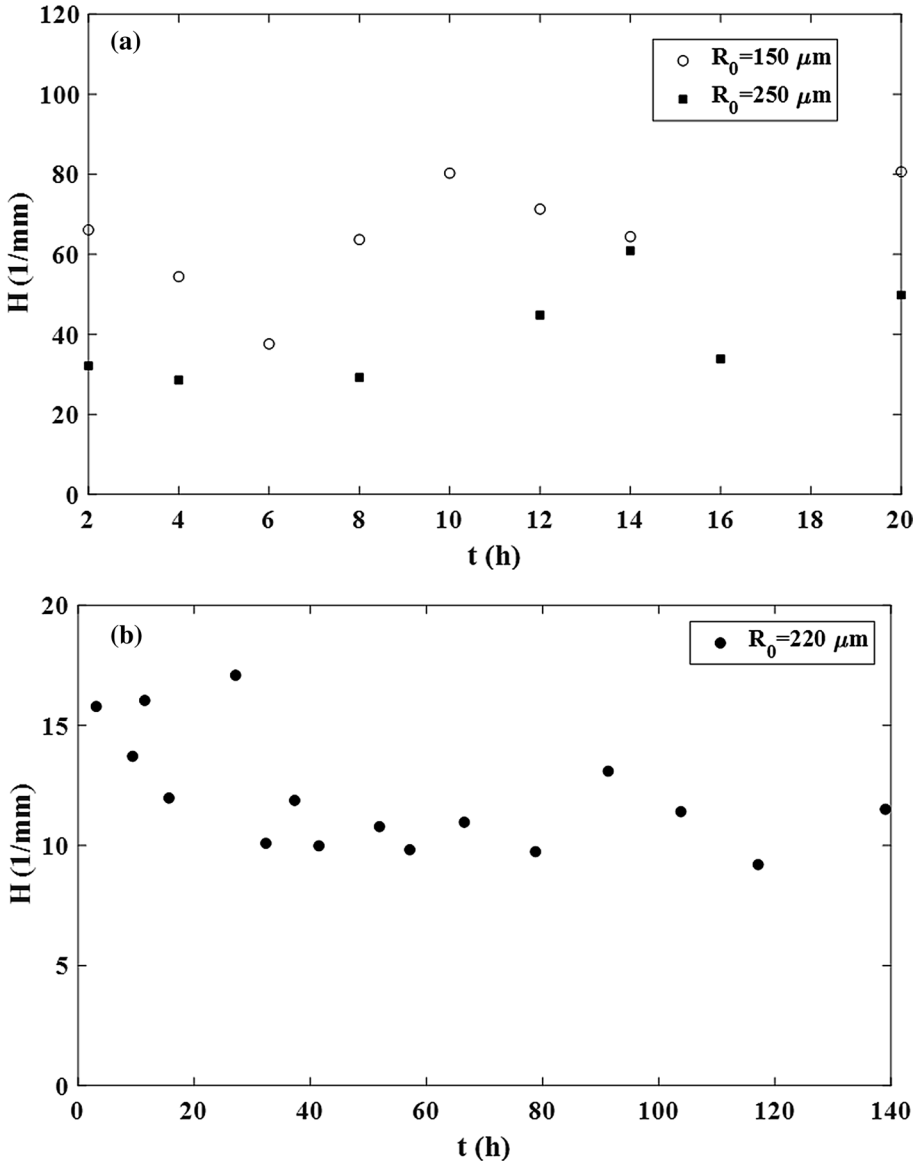

Fig. 3 **a** The curvature of two human carcinoma cell aggregates (HCT116 cell line)- system change during fusion (small and large aggregates). **b** The curvature of two skin fibroblast cell aggregate- system change during fusion

system induces a periodical change of the internal stress σ_i as well as the configuration of migrating cells which have a feedback impact to the tissue surface tension γ.

Periodical change of configuration of migrating cells and the tissue surface tension

Three scenarios of cell migration have been recognized as a consequence of action the viscoelastic force against the surface tension force: (1) most of the cells migrate (the first scenario), (2) some cell groups migrate while the others, at the same time, stay in resting state (the second scenario), and (3) most of the cells stay in the resting state (the third scenario) (Pajic-Lijakovic and MIlivojevic 2017a, 2019c). The viscoelastic force increases as a consequence of residual stress accumulation during CCM which induces local stiffening of multicellular system. This stiffening suppresses cell migration by changing the migrating scenarios (from the first to third) and decreasing the volume fraction of migrating cells. Migrating-to-resting cell state transition, i.e. jamming state transition induces local softening of multicellular system (Pajic-Lijakovic and Milivojevic 2019a, c). It is in accordance with the fact that migrating cells are much stiffer than resting ones due to an accumulation of contractile energy (Lange and Fabry 2013). A local increase in cell packing density which leads to the jamming state transition intensifies the contact inhibition of locomotion (CIL) which has a feedback impact to the state of cell–cell adhesion contacts (Alert and Trepat, 2020). Consequently, CIL induces weakening of cell–cell adhesion contacts which additionally

contribute to the softening of multicellular system parts. This softening leads to a decrease in the viscoelastic force. Then, the surface tension force is capable of inducing CCM again.

These scenarios have been recognized in 2D and 3D CCM as fluctuations of the shape of multicellular systems (Pajic-Lijakovic and Milivojevic 2017a; Pérez-González et al. 2019). Pérez-González et al. (2019) discussed these fluctuations in the context of the wetting model formulated at a cellular level while Pajic-Lijakovic and Milivojevic (2017a) discussed the phenomenon based on the Eyring model formulated at a supracellular level. The viscoelastic force and surface tension force in one hand and the traction force on the other are capable of inducing the wetting to de-wetting transition in 2D multicellular system during CCM. Pajic-Lijakovic and Milivojevic (2017a) considered the cell aggregate rounding after uni-axial compression and quantified by various relaxation rates of the cell aggregate shape k^j. They examined the experimental data by Mombach et al. (2005) and revealed that the relaxation rates k^j (where k^j is the relaxation rate for the j-th cycle) are not random but gather around two or three values indicating various scenarios of cell migration. Three values of the relaxation rates were calculated: (1) k_m- for the first scenario, (2) $k_r \approx 0$ for the third scenario, and (3) $k_r < k_t < k_m$ for the second scenario.

Cell aggregate shape relaxation after uni-axial compression in the form of the aggregate aspect ratio vs. time for the experimental data by Mombach et al. (2005) is shown in the log-normal form (Fig. 4).

Periodical change of the configuration of migrating cells results in the oscillatory change of (1) the curvature of two-aggregate system during fusion (Fig. 3a,b) and (2) the aggregate aspect ratio during aggregate rounding (Fig. 4). This change of the configuration of migrating cells represents the main cause of oscillations of the tissue surface tension $\Delta\gamma(t)$ (where $\Delta\gamma(t) = \gamma(t) - \gamma_0$ is the tissue surface tension difference and γ_0 is the equilibrium value of the surface tension). Pajic-Lijakovic and Milivojevic (2017a, 2019c) formulated the Eyring model for describing successive migrating-to-resting cell state transitions caused by action the viscoelastic force against the surface tension force. It was expressed as (Pajic-Lijakovic and Milivojevic 2017a, 2019c):

$$\frac{d\Delta\gamma_r(t)}{d\tau} = -\lambda_{r\to m}\Delta\gamma_r(t) + \lambda_{m\to r}\Delta\gamma_m(t) \tag{9}$$

where $\Delta\gamma_r(t)$ is the dynamic surface tension contribution from resting cells equal to $\Delta\gamma_r(t) = \gamma_r(t) - \gamma_0$ and $\Delta\gamma_m(t)$ is the dynamic surface tension contribution from migrating cell groups equal to $\Delta\gamma_m(t) = \gamma_m(t) - \gamma_0$. Total dynamic surface tension represents the sum of contributions from migrating and from resting cells, i.e. $\Delta\gamma(t) = \Delta\gamma_m(t) + \Delta\gamma_r(t)$. The specific rate $\lambda_{r\to m}$ (for $r \to m$ transition) was expressed as $\lambda_{r\to m} = \lambda e^{-\frac{\Delta E_B - \Delta E_{eff}}{k_B T_{eff}}}$, λ is the characteristic frequency, k_B is the Boltzmann constant, T_{eff} is the effective temperature (Pajic-Lijakovic and Milivojevic 2017a, 2019c). Concept of effective temperature has been applied for considering rearrangement of various thermodynamic systems from glasses and sheared fluids to granular systems (Casas-Vazquez and Jou 2003). Pajic-Lijakovic and Milivojevic (2019c, 2021a) applied this concept to cell long-timescale rearrangement of dense cellular systems. The effective temperature, in this case, represents a product of cell migration and was expressed as $k_B T_{eff} \sim \langle s \rangle^2$, (where $\langle s \rangle$ is the average cell speed) (Pajic-Lijakovic and Milivojevic 2021a). The

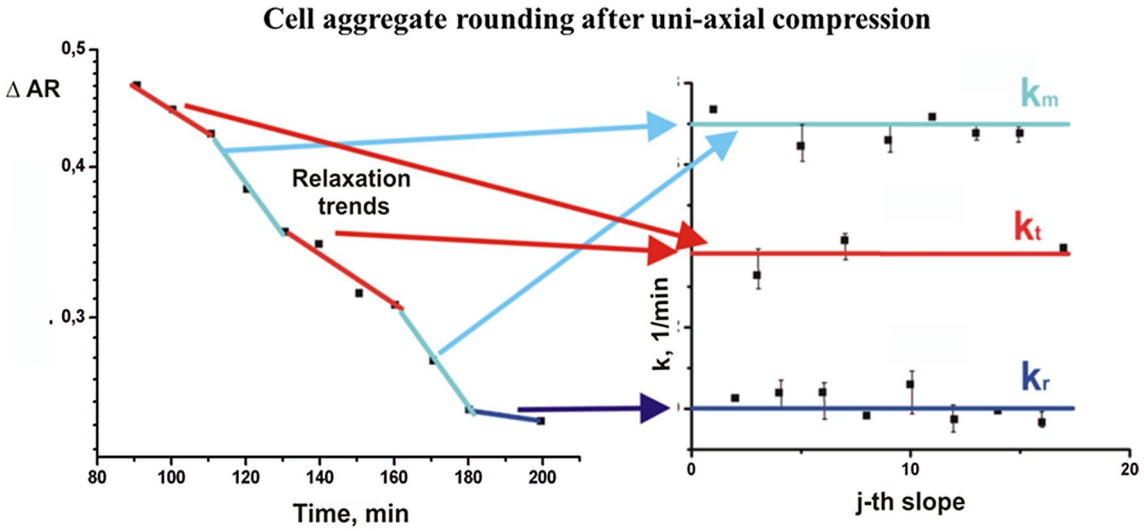

Fig. 4 Cell aggregate shape relaxation after uni-axial compression in the form of the aggregate aspect ratio vs. time

energetic barrier for CCM ΔE_B can be expressed as $\Delta E_B = \langle \sigma_i \varepsilon_V \rangle \Delta V$ (where ΔV is the volumetric change of the aggregate during an increment of time Δt and $\langle \sigma_i \varepsilon_V \rangle$ is the time averaged macroscopic volumetric strain energy). The specific rate for $m \rightarrow r$ transition $\lambda_{m \rightarrow r}$ is expressed as $\lambda_{m \rightarrow r} = \lambda e^{-\frac{\Delta E_B + \Delta E_{eff}}{k_B T_{eff}}}$ (Pajic-Lijakovic and Milivojevic 2017a). The effective driving energy is equal to $\Delta E_{eff} = \gamma_0 \Delta A - \Delta E_p$ (where ΔA is the aggregate surface change during the aggregate rounding or the fusion of two aggregates, ΔE_p is the energy perturbations caused by collision of velocity fronts). The ratio $\frac{\lambda_{r \rightarrow m}}{\lambda_{m \rightarrow r}}$ is equal to $\frac{\lambda_{r \rightarrow m}}{\lambda_{m \rightarrow r}} = e^{-\frac{2\Delta E_{eff}}{k_B T_{eff}}}$ (Pajic-Lijakovic and Milivojevic 2021a). Three causes were established depending on the energy perturbation ΔE_p (Pajic-Lijakovic and Milivojevic 2019c):

(1) $\gamma_0 \Delta A \gg \Delta E_p$ which corresponds to $\lambda_{r \rightarrow m} = \lambda_{m \rightarrow r} e^{-\frac{2\gamma_0 \Delta A}{k_B T_{eff}}}$;
(2) $\gamma_0 \Delta A \sim \Delta E_p$ which corresponds to $\lambda_{r \rightarrow m} \sim \lambda_{m \rightarrow r}$, and.
(3) $\gamma_0 \Delta A \ll \Delta E_p$ which corresponds to $\lambda_{r \rightarrow m} \ll \lambda_{m \rightarrow r}$.

The contribution of resting cells to the tissue surface tension was expressed as $\Delta \gamma_r(t) = E_{app} \Delta AR(t)$, while the contribution of migration cells was expressed as $\Delta \gamma_m(t) = \eta_{app} \frac{d\Delta AR(t)}{d\tau}$ (where $\Delta AR(t)$ is equal to $AR(t) = AR(t) - AR(t \rightarrow \infty)$, $AR(t \rightarrow \infty) \leq 1$, E_{app} is the apparent surface elasticity modulus and η_{app} is the apparent surface viscosity) (Pajic-Lijakovic and Milivojevic 2021a). The $AR(t \rightarrow \infty)$ is $AR(t \rightarrow \infty) \rightarrow 1$ for the aggregate rounding described by Mombach et al. (2005) and for the aggregates fusion described by Shafiee et al. 2015, while for the fusion of two smaller carcinoma aggregates described by Dechristé et al. (2018) $AR(t \rightarrow \infty) < 1$. Change in the ΔAR with time was expressed by introducing expressions for $\Delta \gamma_r(t)$ and $\Delta \gamma_m(t)$ into Eq. 9 as:

$$\frac{d\Delta AR(t)}{dt} + k\Delta AR(t) = 0 \tag{10}$$

where $k = \frac{\lambda_{r \rightarrow m} E_{app}}{E_{app} - \lambda_{m \rightarrow r} \eta_{app}}$ is the aggregate shape relaxation rate. The corresponding relaxation rate is equal to (Pajic-Lijakovic and Milivojevic, 2019c):

(1) $k_m = \frac{\lambda_{m \rightarrow r} e^{-\frac{2\gamma_0 \Delta A}{k_B T_{eff}}} E_{app}}{E_{app} - \lambda_{m \rightarrow r} \eta_{app}}$ for the first scenario,
(2) $k_t = k_m e^{-\frac{2\gamma_0 \Delta A}{k_B T_{eff}}}$ for the second scenario, and.
(3) $k_r \rightarrow 0$ for the third scenario.

The aggregate surface energy $\gamma_0 \Delta A$ relative to a specific energy of collectively migrated cells $k_B T_{eff}$ can be estimated from the experimentally determined ratio of the relaxation rates $\frac{k_m}{k_t}$. Pajic-Lijakovic and Milivojevic (2021a) calculated the ratio $\frac{k_m}{k_t}$ from the experimental data by Mombach et al. (2005). Mombach et al. (2005) examined the aggregate rounding for 3D chicken embryonic neural retina aggregates with various radius: $R = 87\mu m$, and $R = 65\mu m$. The energetic ratio $\frac{\gamma_0 \Delta A}{k_B T_{eff}}$ is estimated as $\frac{\gamma_0 \Delta A}{k_B T_{eff}} = 0.36 \pm 0.04$ for both aggregate sizes (Pajic-Lijakovic and Milivojevic 2019c).

Conclusion

Periodical change of the mechanical parameters (the mechanical waves) such as shape and curvature of multicellular systems, the internal normal stress, and the dynamic tissue surface tension is discussed on two 3D modeling systems such as: (1) the fusion of two-cell aggregates and (2) the cell aggregate rounding after uni-axial compression. The phenomenon has been experimentally confirmed in 2D multicellular systems. However little was reported about the generation of mechanical waves during 3D CCM. This modeling consideration is an attempt to (1) discuss the mechanical waves generation from the standpoint of rheology and (2) point out that the mechanical waves represent the general characteristic of 2D and 3D long-timescale cell rearrangement.

The mechanical waves are a product of the active turbulence occurred at low Reynolds number caused by competition between the viscoelastic force and the surface tension force. The viscoelastic force is the resistive force, while the surface tension force is the driving force for CCM. The viscoelastic force is a product of the residual stress accumulation and its inhomogeneous distribution caused by CCM. An increase in the viscoelastic force leads to a system stiffening which is capable of suppressing the cell movement by changing the configuration of migrating cells and inducing the cell jamming state transition. The following migrating-to-resting cell state transition causes the system softening which results in a decrease in the viscoelastic force. Then, the surface tension force acts to reduce the surface and induces CCM again.

Additional experiments are necessary to correlate the configuration of migrating cells and the rate of its change with the surface free energy and the internal normal stress accumulation for various cell types. These finding could be useful for better understanding various cellular processes such as morphogenesis and cancer invasion.

Acknowledgements This work was supported by the Ministry of Education, Science and Technological Development of the Republic of Serbia (Contract No. 451-03-9/2021-14/200135).

Declarations

Conflict of interest We have no conflict of interest.

References

Alert R, Casademunt J, Joanny J-F (2021) Active turbulence. arXiv: 2104.02122v1

Alert R, Trepat X (2020) Physical models of collective cell migration. Annu Rev Condens Matter Phys 11:77–101

Ban E, Wang H, J. Franklin M, Liphardt JT, Janmey PA, Shenoy VB. (2019) Strong triaxial coupling and anomalous Poisson effect in collagen networks. PNAS 116(4):6790-6799

Barriga EH, Mayor R (2019) Adjustable viscoelasticity allows for efficient collective cell migration. Sem Cell Dev Biol 93:55–68

Blanchard GB, Fletcher AG, Schumacher LJ (2019) The devil is in the mesoscale: mechanical and behavioural heterogeneity in collective cell movement. Sem Cell Dev Biol 93:46–54

Casas-Vazquez J, Jou D (2003) Temperature in non-equilibrium states: a review of open problems and current proposals. Rep Prog Phys 66:1937–2023

Dechristé G, Fehrenbach J, Griseti E, Lobjois V, Clair PC (2018) Viscoelastic modeling of the fusion of multicellular tumor spheroids in growth phase. J Theor Biol 454:102–109

Deforet M, Hakim V, Yevick H, Duclos G, Silberzan P (2014) Emergence of collective modes and tri-dimensional structures from epithelial confinement. Nature Comm 5(1):3747. https://doi.org/10.1038/ncomms4747

Gongora C, Candeil L, Vezzio N, Copois V, Denis V, Breil C, Molina F, Fraslon C, Conseiller E et al (2008) Altered expression of cell proliferation-related and interferon-stimulated genes in colon cancer cells resistant to SN38. Cancer Biol & Therapy 7(6):822–832

Groisman A, Steinberg V (1998) Mechanism of elastic instability in Couette flow of polymer solutions: Experiment. Phys Fluids 10(10):2451–2463

Groisman A, Steinberg V (2000) Elastic turbulence in a polymer solution flow. Nature 405:53–55

Grosser S, Lippoldt J, Oswald L, Merkel M , Sussman DM, Renner F, Gottheil P, Morawetz EW , Fuhs T, Xie X, et al. (2021) Cell and Nucleus Shape as an Indicator of Tissue Fluidity in Carcinoma. Phys Rev X 11, 011033.

Guevorkian K, Gonzalez-Rodriguez D, Carlier C, Dufour S, Brochard-Wyart F (2011) Mechanosensitive shivering of model tissues under controlled aspiration. PNAS 108(33):13387–13392

Kosztin I, Vunjak-Novakovic G, Forgacs G (2012) Colloquium: Modeling the dynamics of multicellular systems: Application to tissue engineering. Rev Mod Phys 84(4):1791–1805

Lange JP, Fabry B (2013) Cell and tissue mechanics in cell migration. Exp Cell Res 319:2418–2423

Lee P and Wolgemuth CW. (2011) Crawling Cells Can Close Wounds without Purse Strings or Signaling. PLoS Comput Biol 7(3):e1002007 1–8.

Marmottant P, Mgharbel A, Kafer J, Audren B, Rieu JP, Vial JC, van der Sanden B, Maree AFM, Graner F, Delanoe-Ayari H (2009) The role of fluctuations and stress on the effective viscosity of cell aggregates. PNAS 106(41):17271–17275

Mc Cann C, Kriebel PW, Parent CA, Losert W (2010) Cell speed, persistence and information transmission during signal relay and collective migration. J Cell Sci 123(10):1724–1731

Mombach JCM, Robert D, Graner F, Gillet G, Thomas GL, Idiart M, Rieu JP (2005) Rounding of aggregates of biological cells: experiments and simulations. Phys A 352:525–534

Mondal S, Phukan M, Ghatak A (2015) Estimation of solid–liquid interfacial tension using curved surface of a soft solid. PNAS 112(41):12563–12568

Nnetu KD, Knorr M, Kaes J, Zink M (2012) The impact of jamming on boundaries of collectively moving weak-interacting cells. New J Phys 14:115012

Notbohm J, Banerjee S, Utuje KJC, Gweon B, Jang H, Park Y, Shin J, Butler JP, Fredberg JJ, Marchetti MC (2016) Cellular contraction and polarization drive collective cellular motion. Biophys J 110(12):2729–2738

Ongenae S, Cuvelier M, Vangheel J, Ramon H, Smeets B (2021) Activity-induced fluidization and arrested coalescence in fusion of cellular aggregates. Front Phys. https://doi.org/10.3389/fphy.2021.649821

Oriola D, Marin-Riera M, Anlas K, Gritti N, Matsumiya M, Aalderink G, Ebisuya M, Sharpe J, Trivedi V (2020) Arrested coalescence of multicellular aggregates. https://arxiv.org/abs/2012.01455

Oswald L, Grosser S, Smith DM, Kaes JA (2017) Jamming transition in cancer. J Phys d: Appl Phys 50(483001):1–17

Pajic-Lijakovic I. (2021) Basic concept of viscoelasticity, in Viscoelasticity and collective cell migration, eds. I. Pajic-Lijakovic and E. Barriga, Chapter 2, Elsevier, ISBN: 9780128203118.

Pajic-Lijakovic I, Milivojevic M (2017a) Successive relaxation cycles during long-time cell aggregate rounding after uni-axial compression. J Biol Phys 43(2):197–209

Pajic-Lijakovic I, Milivojevic M (2017b) Viscoelasticity of multicellular surfaces. J Biomech 60:1–8

Pajic-Lijakovic I, Milivojevic M (2019a) Long-time viscoelasticity of multicellular surfaces caused by collective cell migration—multi-scale modeling considerations. Sem Cell Dev Biol 93:87–96

Pajic-Lijakovic I. and Milivojevic M. (2019b) Functional epithelium remodeling in response to applied stress under in vitro conditions. Appl Bionics Biomech. https://doi.org/10.1155/2019/48927

Pajic-Lijakovic I, Milivojevic M (2019c) Jamming state transition and collective cell migration. J Biol Eng 13:73. https://doi.org/10.1186/s13036-019-0201-4

Pajic-Lijakovic I, Milivojevic M (2020a) Collective cell migration and residual stress accumulation: rheological consideration. J Biomech 108:109898. https://doi.org/10.1016/j.jbiomech.2020.109898

Pajic-Lijakovic I, Milivojevic M (2020b) Mechanical oscillations in 2D collective cell migration: the elastic turbulence. Front Phys. https://doi.org/10.3389/fphy.2020.585681

Pajic-Lijakovic I, Milivojevic M (2021a) Multiscale nature of cell rearrangement caused by collective cell migration. Europ Biophys J 50:1–14

Pajic-Lijakovic I, Milivojevic M (2021b) Viscoelasticity and cell jamming state transition. https://doi.org/10.1101/2021.03.19.436195

Pérez-González C, Alert R, Blanch-Mercader C, Gómez-González M, Kolodziej T, Bazellieres E, Casademunt J, Trepat X (2019) Active wetting of epithelial tissues. Nature Phys 15(1):79–88

Petrolli V, Boudou T, Balland M, Cappello G. (2021) Oscillations in collective cell migration, in Viscoelasticity and collective cell migration, eds. I. Pajic-Lijakovic and E. Barriga, Chapter 8, Elsevier, ISBN: 9780128203118.

Rieu JP, Upadhyaya A, Glazier JA, Ouchi NB, Sawada Y (2000) Diffusion and Deformations of Single Hydra Cells in Cellular Aggregates. Biophys J 79:1903–1914

Serra-Picamal X, Conte V, Vincent R, Anon E, Tambe DT, Bazellieres E, Butler JP, Fredberg JJ, Trepat X (2012) Mechanical waves during tissue expansion. Nature Phys 8(8):628–634

Shafiee A, McCune M, Forgacs G, Kosztin I (2015) Post-deposition bioink self-assembly: a quantitative study. Biofabric 7:045005. https://doi.org/10.1088/1758-5090/7/4/045005

Tambe DT, Croutelle U, Trepat X, Park CY, Kim JH, Millet E, Butler JP, Fredberg JJ. (2013) Monolayer Stress Microscopy: Limitations, Artifacts, and Accuracy of Recovered Intercellular Stresses. PLoS ONE 8(2):e55172 1–13.

Tlili S, Gauquelin E, Li B, Cardoso O, Ladoux B, Delanoë-Ayari H, F Graner F. (2018) Collective cell migration without proliferation: density determines cell velocity and wave velocity. R Soc Open Sci 5:172421, https://doi.org/10.1098/rsos.172421

Tlili S, Durande M, Gay C, Ladoux B, Graner F, Delanoë-Ayari H. (2020) Migrating Epithelial Monolayer Flows Like a Maxwell Viscoelastic Liquid. Phys Rev Lett 125:088102.

Trepat X, Wasserman MR, Angelini TE, Millet E, Weitz DA, Butler JP, Fredberg JJ (2009) Physical forces during collective cell migration. Nature Phys 5:426–430

Tschoegl NW, Knauss WG, Emri I (2002) Poisson's ratio in linear viscoelasticity—a critical review. Mech Time-Depend Mat 6:3–51